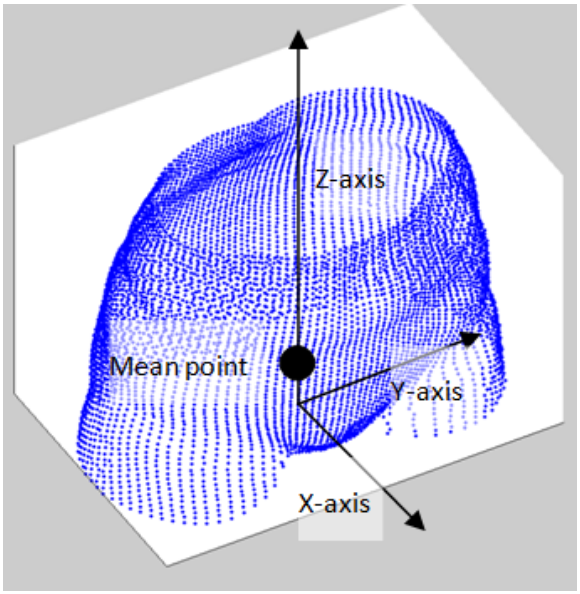

Fig. 3. Waist to hip section of a scanned body surface.

Thirdly, $Point_{aligned}(x,y,z)$ will be converted into Polar coordinate to get $Point_{aligned}(r,\Theta,z)$ (see figure 4 left). It is obvious that the points in point-cloud data are sampled unevenly from the object's surface. However, a uniform distribution of the surface is often required to guarantee a hole-free rendering of the surface [9]. To achieve an even distribution of surface we employ Gridfit method [10]. The Gridfit estimates a surface on a 2d grid, based on scattered data $Point_{aligned}(r,\Theta,z)$. It adopts a modified ridge estimator to generate the surface approximate the $Point_{aligned}(r,\Theta,z)$, where the bias is toward smoothness. It is not an interpolant. Its goal is a smooth surface which is similar to the human surface shown as figure 5. The 201X101 sized evenly distributed grid on surface has 20301 intersection points, and the location of these points, $Point_{grid}(r,\Theta,z)$, are regarded as the sampled point for shape map data.

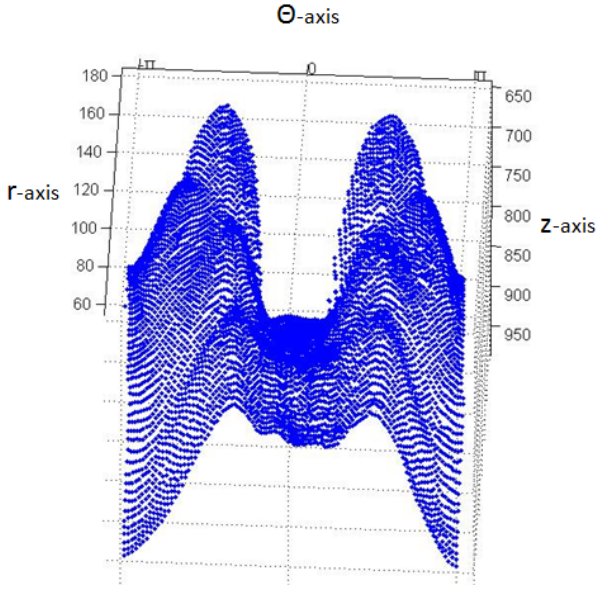

Fig. 4. $Point_{aligned}(r,\Theta,z)$ in 3D space.

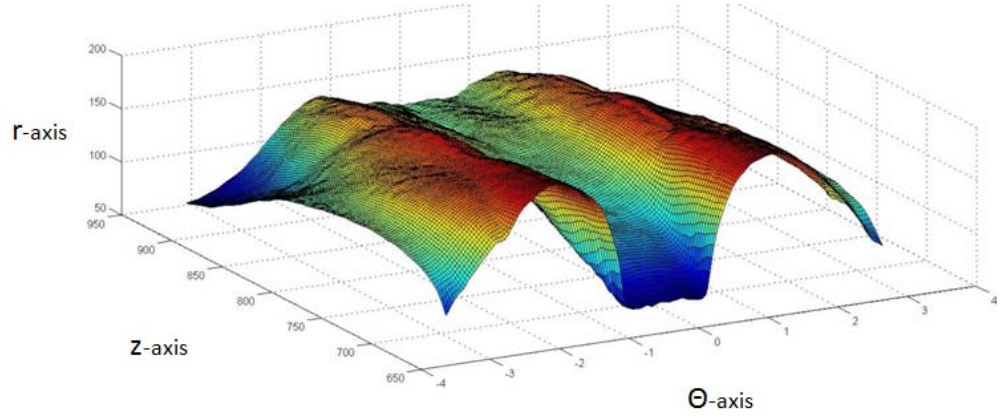

Fig. 5. Point$_{aligned}$(r,Θ,z) in 3D space.

Finally, a PNG file is created to store the Point$_{grid}$(r,Θ,z) in the form of gray level value. To achieve this, we converted the Point$_{grid}$(r,Θ,z) into a 2D matrix ShapeMap(x',y'), which is defined as

$$x' = \frac{\Theta + \pi}{\mathrm{Step}_x} + 1 \qquad (3)$$

$$y' = \frac{\mathrm{z\text{-}min(z)}}{\mathrm{Step}_y} + 1 \qquad (4)$$

$$ShapeMap(x', y') = r * 100 \qquad (5)$$

Where Step$_x$ is the length of each grid in Θ-axis direction, whose default value is 0.0314. Step$_y$ is the length of each grid in z-axis direction, whose default value is (max(z)-min(z))/100 . The value of ShapeMap(x',y') is 100 times of the value of r then rounded to nearest integer. The reason to magnify its value by 100 times is to reserve the precision to percentile when converted to a gray level value which must be an integer.

2.1.1. Shape map PNG file specification

Figure 6 shows an example of shape map PNG file. It contains two main parts: the caption and shape map value (see figure 7). The caption part contains the file name and the value of min (z) and max (z) described in section 2.1. The ShapeMap(x',y') value is stored as the 16 bit gray level value for the PNG file.

Fig. 6. PNG file: G1_684.8125_946.3625

101	ShapeMap(1,101)	...	...	...	ShapeMap(201,101)
⋮	⋮	...	...	...	⋮
2	⋮	...	...	...	⋮
1	ShapeMap(1,1) value range: [0,65535]	...	...	...	ShapeMap(201,1)
y' \ x'	1	2	3	...	201

Caption: file name_min (z)_max (z)

Fig. 7. Shape map PNG layout

2.2. From shape map data to point-cloud data

To retrieve the body scanning point-cloud data from a shape map PNG file, the caption and shape map value must be read to obtain: ShapeMap(x',y'), file name, min(z), max(z). Refer to section 2.1, the point-cloud data Point$_{grid}$(r,Θ,z) can be obtained as following:

$$r = ShapMap(x', y') \qquad (6)$$

$$\Theta = -\pi + (x' - 1) * Step_x \qquad (7)$$

$$z = \min(z) + (y' - 1) * Step_y \qquad (8)$$

And the $Point_{grid}(x'',y'',z'')$ can be obtained by converting the Polar coordinate's values of $Point_{grid}(r,\Theta,z)$ to Cartesian coordinate's values.

3. Results and discussion

We tested the shape map method by converting point-cloud data of waist to hip body section of 75 individuals using the $[TC]^2$ 3D scanner with the Matlab modules. It took 95.4 seconds to convert the whole set of point-cloud data to shape map data, average 1.3 seconds per sample. While it took 15.2 seconds to retrieve the point-cloud data from the shape map data, average 0.2 seconds per sample on a PC with Inter(R) Core(TM) Duo CPU E8500@ 3.16GHz and 4.00 GB memory installed.

The results show that the shape map PNG files set occupied only 12.0% of the storage room for Point-cloud ASCII text (TXT) files. And it contained more sampling points, which was 3.66 times of the original files averagely. By decreasing the value of $Step_x$ and $Step_y$, it can increase resolution further, but the size of the shape map PNG file will increase simultaneously.

Table 1. Comparison between point-cloud format and shape map format.

	Point-cloud format	Shape map format
Storage room	16.30 MB (average 0.217 MB per file)	1.95 MB (average 0.026 MB per PNG file)
Sampled point	average 5550 unevenly distributed points	20,301 evenly distributed points

Another advantage for the shape map is that it presents the human scanning file in graphic, which is more intuitive than number. For example, the figure 8 shows two shape map files for sample A and B. It is visualized that the size of A is bigger than B as the overall brightness of A is higher than B, and A has a more obvious belly as the lower middle section of A is brighter compared to the surrounding area.

Refer to sections 2.1 and 2.2, the Gridfit method ensures that the original sample points $Point_{aligned}(x,y,z)$ are on the estimated surface, but the original points cannot be accessed directly. It needs to be interpolated using the 4 surrounding $Pointgrid(x'',y'',z'')$.

Fig. 8. Two shape map files: A (upper) and B (lower)

4. Future work

The shape map converting module has been developed in Matlab, however it is designed to convert one part of the body each time (see figure 1 right). Our future work involves the design of a higher level module to work with the full body scanning files by joining all the parts back.

Acknowledgement

The authors would like to acknowledge the support from General Research Fund (GRF) projects HK, B- Q26H and The Hong Kong Polytechnic University Funding U894.

References

1. Z. Ping, (2008): "Hip Circumference Is the Critical Horizontal Part That Affects Female Clothes for Heavy-bust and Slim-waist Figures [J]," Journal of Liaodong University (Natural Science), vol. 2.
2. M. Holewun and W. Lotens., (1992): "The influence of backpack design on physical performance," Ergonomics, vol. 35, pp. 149-157.
3. T. Ryu, et al., (2004): "Development and application of a generation method of human models for ergonomic product design in virtual environment," pp. 951-955.
4. S. M. Carcone and P. J. Keir., (2007):"Effects of backrest design on biomechanics and comfort during seated work," Applied ergonomics, vol. 38, pp. 755-764.
5. F. Segovia, et al., (2011): "A comparative study of feature extraction methods for the diagnosis of Alzheimer's disease using the ADNI database," Neurocomputing.
6. T. Sha, et al., (2011): "Feature level analysis for 3D facial expression recognition," Neurocomputing.
7. E. Paquet, (2004): "Exploring anthropometric data through cluster analysis," .
8. M. Petrov, et al., (1998): "Optical 3D digitizers: Bringing life to the virtual world," Computer Graphics and Applications, IEEE, vol. 18, pp. 28-37.
9. T. Weyrich, et al., (2004): "Post-processing of scanned 3D surface data,".
10. J. U. G. D'Errico, 2006. (Accessed 2009): http://www.mathworks.com/matlabcentral/fileexchange/8998.